

See discussions, stats, and author profiles for this publication at: <https://www.researchgate.net/publication/257355361>

Comment on "Tuning Magnetic Moments by 3d Transition-Metal-Doped Au-6 Clusters"

ARTICLE in THE JOURNAL OF PHYSICAL CHEMISTRY C · DECEMBER 2009

Impact Factor: 4.77 · DOI: 10.1021/jp9074256

CITATIONS

18

READS

26

4 AUTHORS, INCLUDING:



Minh Tho Nguyen

University of Leuven

748 PUBLICATIONS 10,835 CITATIONS

SEE PROFILE



Peter Lievens

University of Leuven

278 PUBLICATIONS 4,588 CITATIONS

SEE PROFILE



Tamás Veszprémi

Budapest University of Technology and Ec...

196 PUBLICATIONS 2,295 CITATIONS

SEE PROFILE

Comment on “Tuning Magnetic Moments by 3d Transition-Metal-Doped Au₆ Clusters”

Tibor Höltzl,^{†,§,||} Peter Lievens,^{‡,§} Tamás Veszprémi,^{||} and Minh Tho Nguyen^{*,†,§}

Department of Chemistry, Laboratory of Solid State Physics and Magnetism, Institute for Nanoscale Physics and Chemistry-INPAC, Katholieke Universiteit Leuven, B-3001 Leuven, Belgium, and Department of Inorganic and Analytical Chemistry, Budapest University of Technology and Economics, Szent Gellért tér 4. H-1521 Budapest, Hungary

Received: August 1, 2009

In a recent article, Zhang et al.¹ showed that the most stable isomer of the transition metal-doped gold clusters Au₆M, with M = Sc, Ti, V, Cr, Mn, Fe, Co, and Ni, consists of a six-membered ring of gold atoms with the dopant at its center. On the basis of an analysis of the calculated density of states and projected density of states, these authors concluded that the d-orbitals of the dopant element stabilize this particular arrangement of the constituent atoms. Also, they confirmed that the magnetic moment of the cluster can be tuned by the incorporation of different dopant atoms,² which renders these clusters perfectly applicable in the design of nanomagnets. Nevertheless, the authors¹ have not analyzed the electronic states and geometries of the doped clusters in terms of the available models.

In this comment, we wish to demonstrate that the stability of the quartet state and the D_{6h} point group of Au₆Mn can be explained using an extension of the phenomenological shell model of metal clusters. Au₆Mn is situated in the middle of the transition metal series and can thus be considered as a representative from which the electronic configurations of others can be built up in both directions. In fact, the model provides a consistent rationalization for the observed variation of the preferred spin states of the Au₆M clusters.

The phenomenological shell model of metal clusters (PSM) was developed to rationalize the observed stability of metal clusters when the number of the itinerant electrons corresponds to a so-called magic number.³ Alkaline metal clusters are particularly stable for cluster sizes of 2, 8, 20, ... atoms.⁴ The main assumption of the PSM is that the itinerant electrons move in an average potential that confines them according to the cluster shape. As in the case of nearly spherical clusters, the molecular orbitals corresponding to the itinerant electrons (called shell orbitals) have shapes similar to that of the atomic orbitals, hence they are denoted by capital S, P, D, ... letters. However, in this case the confining potential does not restrict the azimuthal quantum number for each principal quantum number. In a nearly spherical cluster shape, the energetic order of the shell orbitals is 1S, 1P, 1D, 2S, and so forth. Extended stability is expected for closed electronic structures of 1S², 1S²1P⁶, or 1S²1P⁶1D¹⁰2S².

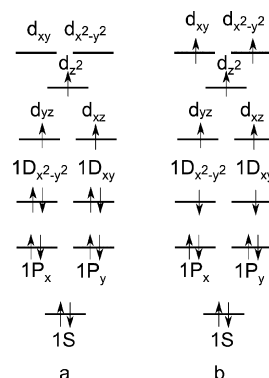
As the number of the corresponding valence electrons equals to 2, 8, 20, respectively, this model fully accounts for the observed magic numbers. In alkaline metal clusters, the valence s electrons are itinerant. In coinage metals, extended stability is expected when the number of the valence s electrons corresponds to a magic number. Hence MOs having relatively high contribution from the valence s AOs are the shell orbitals. However, valence d AOs can also contribute to these shell orbitals. Details of the cluster geometric structure may strongly influence the average potential and thus also will alter the shell orbital energetic ordering, as has been illustrated for a number of binary clusters.⁵

The PSM was also generalized to planar clusters.⁶ The Au₆(D_{6h}) ring has a nearly cylindrical symmetry. The schematic shape, notation, and qualitative energetic ordering of the orbitals of this cluster are shown in Figure 1. As each gold atom possesses one valence s electron, the total number of the itinerant electrons is 6 and hence the electron configuration of this compound is 1S²1P_x²1P_y², while the in-plane 1D and 1F orbitals are unoccupied.

A Mn atom has a 4s²3d⁵ electron configuration, which results in a sextet ground state depicted in Figure 1. If this electronic state is placed in the center of the Au₆ ring, the zeroth-order effect is the splitting of the degenerate d levels (Figure 1). The in-plane d orbitals are stabilized as compared to the d_{xz}, d_{yz}, and d_{z²} orbitals. This is analogous to a crystal field splitting. In the next step, these orbitals combine with the shell orbitals of Au₆. Combination of the 1S shell orbital of Au₆ and the 3s AO of Mn yields the 1S and 2S shell orbitals of Au₆Mn. Similarly, the in-plane 1D shell orbitals of Au₆ and the in-plane d AOs of Mn combine with each other. Distribution of 13 electrons in these orbitals gives rise to a quartet electronic structure, in agreement with the findings of Zhang et al.¹ As shown in Figure 1, the unpaired electrons are more localized on the d AOs of the manganese element. The remaining 10 electrons are itinerant and then occupy the shell orbitals with a 1S²1P_x²1P_y²1D_{xy}²1D_{x²-y²}² electron configuration. This corresponds to a closed electronic structure and also satisfies the Hückel rule. Hence, similarly to the stable planar seven-membered ring Cu₇Sc,⁷ the planarity, stability, and high symmetry of Au₆Mn can simply be explained by its closed electronic shell.

To test the applicability of the above model, we have carried out quantum chemical calculations using the unrestricted UBP86 functional and complete active space self-consistent field (CASSCF) method in conjunction with the Stuttgart–Dresden

SCHEME 1



* To whom correspondence should be addressed. E-mail: minh.nguyen@chem.kuleuven.be.

[†] Department of Chemistry, Katholieke Universiteit Leuven.

[‡] Laboratory of Solid State Physics and Magnetism, Katholieke Universiteit Leuven.

[§] INPAC, Katholieke Universiteit Leuven.

^{||} Budapest University of Technology and Economics.

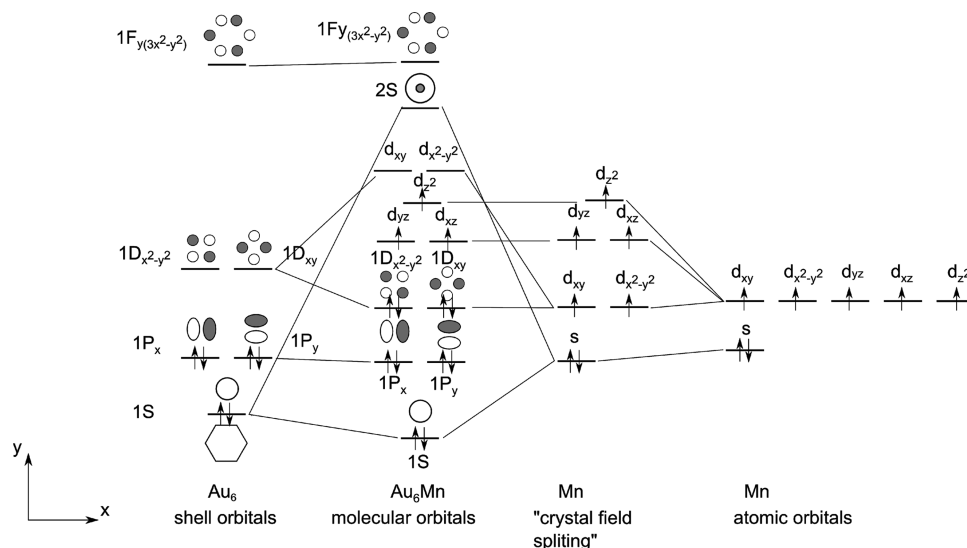


Figure 1. Schematic orbital diagram of Au_6Mn and its Au_6 and Mn constituents. Orientation of the x and y coordinate axes are showed in the figure, while the z axis is perpendicular to them. Shell orbitals are denoted by capital letters, while atomic orbitals are labeled by lower case letters.

(SDD) basis set and small core relativistic pseudopotentials. All computations were done with the aid of the Gaussian 03 program package.⁸ The active space of CASSCF computations involves 13 electrons and 12 orbitals as depicted in Figure 1. The isosurfaces of the resulting natural orbitals and their occupations are summarized in Figure 2.

As shown in Figure 2, both DFT and CASSCF methods give similar electron occupations for these orbitals. As expected, the $1s$, $1p_x$, and $1p_y$ orbitals are doubly occupied, while the spin up unpaired electrons are located on the $1d_{xz}$, $1d_{yz}$, and $1d_{z^2}$ orbitals of Mn. However the populations of the $1d_{xy}$ and $1d_{x^2-y^2}$ orbitals are smaller than the expected 2.0, while that of the $3d_{xy}$ and $3d_{x^2-y^2}$ orbitals is larger than 0.0.

This shows that the ground state of Au_6Mn can be described by two configurations displayed in Scheme 1. Configuration a corresponds to the one shown in Figure 1, while configuration b corresponds to an overall quartet state with two spin down and five spin up electrons. In the canonical molecular orbital picture, configuration b is occupied and was analyzed in detail in ref 2. These configurations are consistent with the calculated local magnetic moment of the Mn atom ($4.277 \mu_B$),¹ which is between the values expected from configurations a and b. A corollary of the existence of two configurations is that the local magnetic moment of the central manganese atom is larger than 3, and the excess magnetic moment is compensated by the Au_6 ring. This is similar to the Kondo-effect⁹ observed in solid state, where the magnetic moment of an impurity magnetic center is quenched by the surroundings. A similar effect was also observed in the case of the $\text{Au}_{10}\text{Co}^+$ cluster,¹⁰ where the magnetic moment of the cobalt atom is completely quenched by the surrounding gold atoms.

In the case of transition metal atoms, the energy ordering of the orbitals, and hence the electronic configuration, strongly depends on the system considered. For example, the ground state of the vanadium element is $[\text{Ar}]3d^34s^2$, while in the chromium atom it is $[\text{Ar}]3d^54s^1$. Similar to the present case, occupation of the orbitals depicted in Figure 1 also depends on the impurity atoms. However some general considerations can be drawn from the previous discussion. By adding electrons to, or subtracting electrons from, the d_{xy} , $d_{x^2-y^2}$, d_{xz} , or d_{yz} orbitals, the system will have differently occupied degenerate orbitals, and as a consequence, it undergoes a Jahn–Teller distortion.

This is indeed the case for Au_6Cr . As this system has one electron less than Au_6Mn , one electron is thus subtracted from the $1d_{xy}$ or $1d_{x^2-y^2}$ orbital, hence the occupation of the d_{xz} and d_{yz} is also changed. The result is that the system distorts to lower symmetry. According to configuration b in Scheme 1, a spin down electron is removed and the resulting total magnetic moment amounts to $4\mu_B$, which was effectively observed.¹

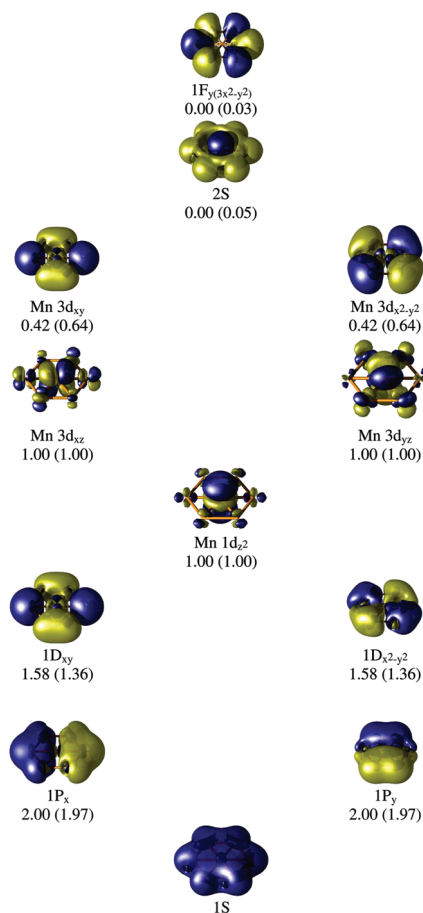


Figure 2. Natural orbitals of Au_6Mn corresponding to the MOs depicted in Figure 1. Occupations are obtained using BP86/SDD and CASSCF(13,12)/SDD (in parentheses) levels of theory.

Au₆Fe has one more valence electron compared to Au₆Mn. This excess electron makes the d_{yz} orbital doubly occupied, while the d_{xz} orbital remains singly occupied. This electron distribution again results in a Jahn–Teller distortion that lowers the cluster symmetry. Also, the spin state is reduced to a triplet, which was indeed found.¹ Similar effects were found in the case of Au₆X[−] anions (ref 2).

In the case of Au₆Sc D_{6h} symmetry was reported by Zhang et al. As the valence d electron of scandium is also itinerant this compound has 9 shell electrons, therefore according to the previous model the suggested D_{6h} symmetry is unexpected. Our computations showed that the D_{6h} symmetry structure relaxes to D_{2h} symmetry. The resulting compound still has one normal mode with imaginary frequency which yields a C_{2v} symmetry structure upon relaxation. This cluster has the 1S² 1P_x² 1P_y² 1D_{xy}² 1D_{x²−y²¹ occupation, which is in agreement with the previous model of the electronic structure. This occupation also leads to a Jahn–Teller instability in D_{6h} symmetry. A similar structure was observed in the case of the isovalent Au₆Y.¹¹}

We would like to point out that the simple model presented here is able to describe and predict the electronic structure of the Au₆M species, and it is also expected to be useful for the study of other types of doped metal clusters. In addition, the electronic mechanism of how the Au₆ ring can host a transition metal dopant atom can be understood.

References and Notes

(1) Zhang, M.; He, L.-M.; Zhao, L.-X.; Feng, X.-J.; Luo, Y.-H. *J. Phys. Chem. C* **2009**, *113*, 6491.

- (2) Li, X.; Kiran, B.; Cui, L.-F.; Wang, L.-S. *Phys. Rev. Lett.* **2005**, *95*, 253401.
- (3) De Heer, W. A. *Rev. Mod. Phys.* **1993**, *65*, 611.
- (4) Knight, W. D.; Clemenger, K.; de Heer, W. A.; Saunders, W. A.; Chou, M. Y.; Kohen, M. L. *Phys. Rev. Lett.* **1984**, *52*, 2141. and 1984, *53*, 510.
- (5) Janssens, E.; Neukermans, S.; Lievens, P. *Curr. Opin. Solid State Mater. Sci.* **2004**, *8*, 185, and references therein.
- (6) Janssens, E.; Tanaka, H.; Neukermans, S.; Silverans, R. E.; Lievens, P. *New J. Phys.* **2003**, *5*, 46.1.
- (7) Höltzl, T.; Janssens, E.; Veldeman, N.; Veszprémi, T.; Lievens, P.; Nguyen, M. T. *ChemPhysChem* **2008**, *9*, 833.
- (8) Frisch, M. J.; Trucks, G. W.; Schlegel, H. B.; Scuseria, G. E.; Robb, M. A.; Cheeseman, J. R.; Montgomery, J. A., Jr.; Vreven, T.; Kudin, K. N.; Burant, J. C.; Millam, J. M.; Iyengar, S. S.; Tomasi, J.; Barone, V.; Mennucci, B.; Cossi, M.; Scalmani, G.; Rega, N.; Petersson, G. A.; Nakatsuji, H.; Hada, M.; Ehara, M.; Toyota, K.; Fukuda, R.; Hasegawa, J.; Ishida, M.; Nakajima, T.; Honda, Y.; Kitao, O.; Nakai, H.; Klene, M.; Li, X.; Knox, J. E.; Hratchian, H. P.; Cross, J. B.; Bakken, V.; Adamo, C.; Jaramillo, J.; Gomperts, R.; Stratmann, R. E.; Yazyev, O.; Austin, A. J.; Cammi, R.; Pomelli, C.; Ochterski, J. W.; Ayala, P. Y.; Morokuma, K.; Voth, G. A.; Salvador, P.; Dannenberg, J. J.; Zakrzewski, V. G.; Dapprich, S.; Daniels, A. D.; Strain, M. C.; Farkas, O.; Malick, D. K.; Rabuck, A. D.; Raghavachari, K.; Foresman, J. B.; Ortiz, J. V.; Cui, Q.; Baboul, A. G.; Clifford, S.; Cioslowski, J.; Stefanov, B. B.; Liu, G.; Liashenko, A.; Piskorz, P.; Komaromi, I.; Martin, R. L.; Fox, D. J.; Keith, T.; Al-Laham, M. A.; Peng, C. Y.; Nanayakkara, A.; Challacombe, M.; Gill, P. M. W.; Johnson, B.; Chen, W.; Wong, M. W.; Gonzalez, C.; Pople, J. A. *Gaussian 03*, revision D.02; Gaussian, Inc.: Wallingford, CT, 2004.
- (9) Kondo, J. *Prog. Theor. Phys.* **1964**, *32*, 37.
- (10) Janssens, E.; Neukermans, S.; Nguyen, H. M. T.; Nguyen, M. T.; Lievens, P. *Phys. Rev. Lett.* **2005**, *94*, 113401.
- (11) Lin, L.; Höltzl, T.; Gruene, P.; Claes, P.; Meijer, G.; Fielicke, A.; Lievens, P.; Nguyen, M. T. *Chem. Phys. Chem.* **2008**, *9*, 2471.

JP9074256